

# Transforming the Accuracy and Numerical Stability of ReaxFF Reactive Force Fields

David Furman<sup>\*,†,‡</sup> and David J. Wales<sup>\*,†</sup>

*†Department of Chemistry, University of Cambridge, Lensfield Road, Cambridge CB2  
1EW, United Kingdom*

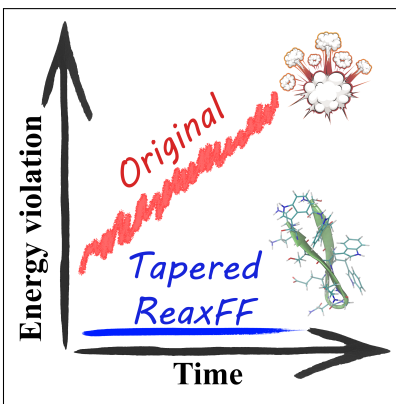
*‡Division of Chemistry, NRCN, P.O. Box 9001, Beer-Sheva 84190, Israel*

E-mail: df398@cam.ac.uk; dw34@cam.ac.uk

## Abstract

Molecular dynamics (MD) simulations provide an important link between theories and experiments. While *ab initio* methods can be prohibitively costly, the ReaxFF force field has facilitated *in silico* studies of chemical reactivity in complex, condensed-phase systems. However, the relatively poor energy conservation in ReaxFF MD has either limited the applicability to short time scales, in cases where energy propagation is important, or has required a continuous coupling of the system to a heat bath. In this study, we reveal the root cause of the unsatisfactory energy conservation, and offer a straightforward solution. The new scheme results in orders of magnitude improvement in energy conservation, numerical stability, and accuracy of ReaxFF force fields, compared to the previous state-of-the-art, at no additional cost. We anticipate that these improvements will open new avenues of research for more accurate reactive simulations in complex systems on long time scales.

## Graphical TOC Entry



Until recently, simulations of chemical reactivity were exclusively dealt with using quantum mechanical approaches. Such treatments severely limited the system size and accessible time scales. The development of the ReaxFF reactive force field has been a significant methodological advance, which provided a new tool for atomistic simulations in computational molecular science. By exploiting a mapping between bond distance and bond order,<sup>1</sup> together with sophisticated many-body correction terms, ReaxFF allows us to describe different bonding environments (covalent, molecular, metallic, and inorganic) on an equal footing. Furthermore, dynamic partial charge partitioning schemes<sup>2-4</sup> allow us to account for polarisation and charge transfer during chemical reactions. A single, properly parameterised ReaxFF force field<sup>5-9</sup> can reach excellent accuracy for structural and energetic features in many challenging systems compared to *ab initio* methods. Moreover, ReaxFF is significantly less costly than DFTB<sup>10</sup> or neural network potentials.<sup>11</sup> Noteworthy applications of ReaxFF include the study of combustion and fuels chemistry,<sup>12-14</sup> heterogeneous catalysis,<sup>15-17</sup> nanotechnology,<sup>18-22</sup> enzymatic reactions,<sup>23</sup> high-energy materials,<sup>24-32</sup> and aqueous phase chemistry,<sup>33-36</sup> among others.

Despite its wide applicability and popularity, energy conservation in ReaxFF MD is inferior compared to non-reactive force fields. Although thermostats can be used to keep the average temperature fixed during equilibration runs, poor energy conservation severely degrades the accuracy of any (long enough) trajectory in the microcanonical ensemble.

In this Letter, we identify and analyse the problem of poor energy conservation in ReaxFF, and suggest simple modifications to the formalism, as well as to several run-time parameters. Key to our analysis is Energy Landscape Theory,<sup>37,38</sup> which analyses the relationships between stationary points on the multidimensional PES and observable properties. Geometry optimisation algorithms, which are central in the Computational Potential Energy Landscape perspective, are highly sensitive probes of the underlying potential energy surface (PES), since they rapidly highlight unphysical features, such as stationary points of the wrong Hessian index, a bad condition number, or presence of discontinuities. Once identi-

fied, such features and their possible effects can be thoroughly investigated.<sup>39</sup> Notably, such sensitivity to the PES topography is seldom evident in standard MD or monte carlo (MC) simulations, which tend to be much more “forgiving” of such fatalities. Hence, potentially detrimental features of the landscape can be missed.

We begin our analysis, which is based on the reference code by van Duin,<sup>16</sup> with several benchmark systems for subsequent geometry optimisation using the highly robust L-BFGS algorithm.<sup>40–42</sup> The chosen structures vary in complexity and have published parameterisations. The systems, together with their respective force fields, are: a van der Waals dimer of 2,4,6-trinitrotoluene (TNT),<sup>27</sup> alanine dipeptide,<sup>43</sup> cyanoethylene and cyclopentadiene (Diels-Alder reactants)<sup>25</sup> and tryptophan zipper 2 (trpzip2) peptide.<sup>43, 44</sup> Lastly, we consider three more challenging systems: bulk liquid water,<sup>34</sup> a single crystal of TNT<sup>27</sup> (orthorhombic polymorph, dimensions:  $14.991 \times 12.154 \times 20.017$ ) and a single crystal of Benzene<sup>45</sup> (orthorhombic polymorph I, dimensions:  $14.888 \times 19.100 \times 13.840$ ).

The outcome of these calculations is summarised in Table 1. The results clearly demonstrate how geometry optimisation using ReaxFF force fields for different systems can be problematic. In five out of seven cases, we have been unable to converge the structure to a local minimum, for which we require a root-mean-squared gradient (RMSG) of  $10^{-6}$  kcal mol<sup>-1</sup> Å<sup>-1</sup> or less. Starting with relatively simple systems: alanine dipeptide (22 atoms) and TNT dimer (42 atoms), the RMSG values (in kcal mol<sup>-1</sup> Å<sup>-1</sup>) of the final structures were  $4.15 \times 10^{-1}$  and  $6.70 \times 10^{-2}$ , respectively. The trpzip 2 system (220 atoms), which has more soft degrees of freedom, and bulk liquid water system (384 atoms), could not be refined below an RMSG of 1.45 and  $8.27 \times 10^{-3}$ , respectively, indicating that the structures are not close to a local minimum. A similar situation is encountered with the TNT crystal, which reaches a final RMSG value of 0.51. The impressive convergence of the Diels-Alder (19 atoms) and Benzene crystal (168 atoms) systems should probably be regarded as success for the robust performance of the L-BFGS algorithm, even for slightly noisy or ill-conditioned landscapes.<sup>41</sup>

The ReaxFF total energy expression contains over a dozen components, including both

**Table 1: Total energies ( kcal mol<sup>-1</sup>) and lowest RMSG ( kcal mol<sup>-1</sup> Å<sup>-1</sup>) achieved for several systems following L-BFGS geometry optimisation.**

System	Final Energy ( kcal mol <sup>-1</sup> )	RMSG ( kcal mol <sup>-1</sup> Å <sup>-1</sup> )
TNT vdW dimer	$-4.88 \times 10^3$	$6.70 \times 10^{-2}$
TNT crystal	$-3.97 \times 10^4$	0.51
Alanine dipeptide	$-2.30 \times 10^3$	$4.15 \times 10^{-1}$
Diels-Alder reactants	$-2.37 \times 10^3$	$9.35 \times 10^{-9}$
trpzip2 peptide	$-2.53 \times 10^3$	1.45
liquid water	$-3.38 \times 10^4$	$8.27 \times 10^{-3}$
Benzene crystal	$-1.00 \times 10^4$	$0.95 \times 10^{-6}$

bonded and non-bonded terms. A careful comparison between the analytic and numerical derivatives of the various energy contributions revealed that, besides the long-range terms, practically all analytic partial gradients disagreed with the numerical values (calculated by a standard central finite-difference scheme).

In ReaxFF, each valence term is made bond order dependent to allow smooth transitions in energies and forces during bond making and breaking. This foundation lies at the heart of the design philosophy. Due to the complexity of the ReaxFF force field, we will first illustrate our analysis for a N<sub>2</sub> molecule with the energetic materials force field.<sup>25</sup> N<sub>2</sub> is the simplest system that spans the whole range of bond orders (i.e. starting from a triple covalent bond up to full dissociation), and does not contain any additional valence terms aside from the bond energy and related coordination corrections. ReaxFF includes long-range interactions between bonded atoms, and irrespective of connectivity, shielded van der Waals (vdW) and Coulomb interactions are calculated between each pair of atoms. Together with the bond energy, they constitute the two-body interactions in the system. Starting with the equilibrium structure, we performed a series of bond compression/expansion experiments, and calculated the corresponding potential energy and RMSG for each configuration, as a function of bond length (Figure 1).

Figure 1a shows that, while some energy contributions for N<sub>2</sub> appear smooth and continuous, the bond energy features a cusp at approximately 2.5 Å, which clearly breaks differentiability at this point, and renders the gradient discontinuous. The vdW energy, which is

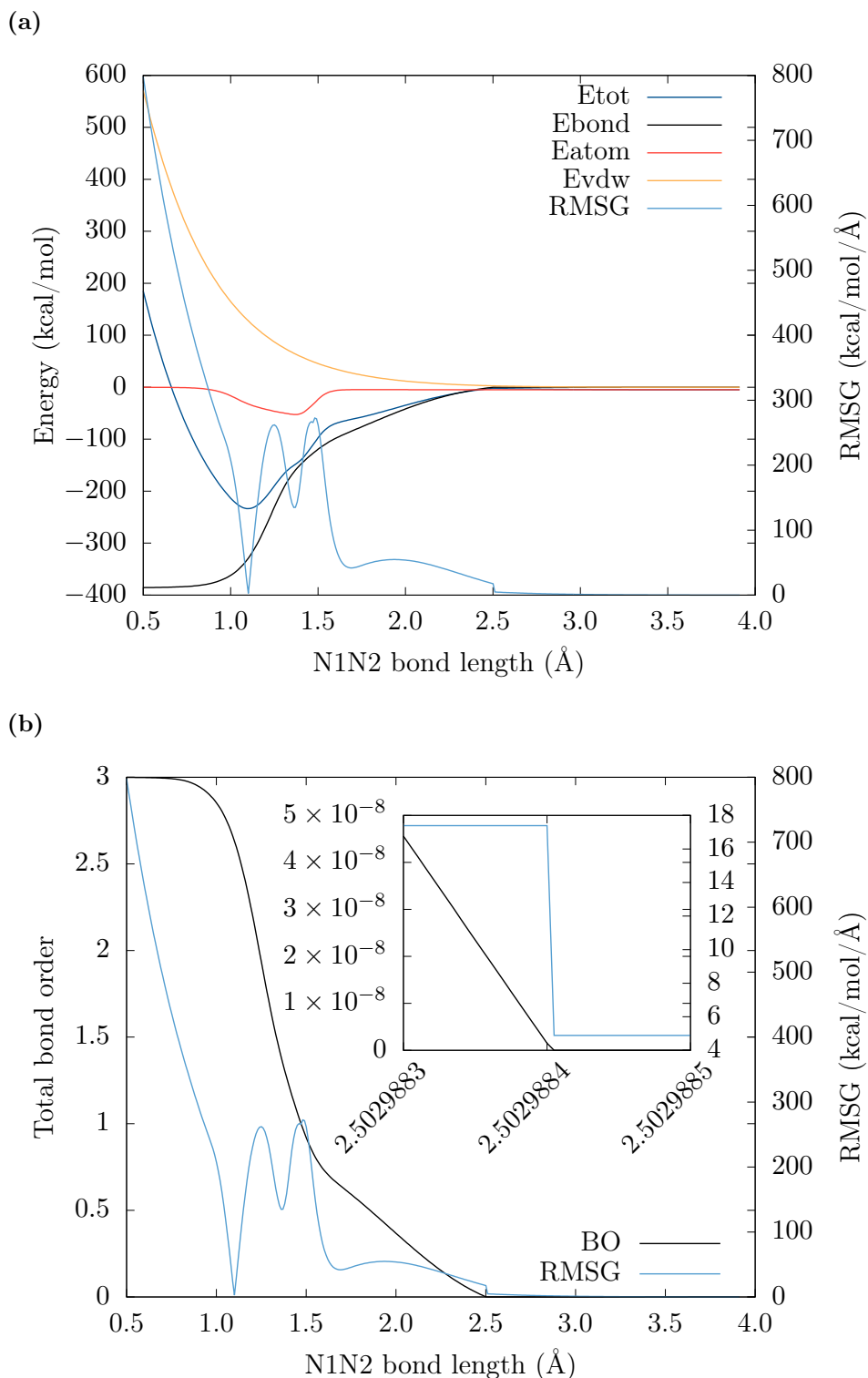


**Figure 1.** Bond compression and expansion curves for molecular  $N_2$ . (a) Potential energy contributions in the system. Total energy (blue line), Bond energy (black line), Atom energy (orange line), vdW energy (yellow line), and RMSG (cyan line). (b) Total bond order (black line), and RMSG (cyan line). The inset focuses on a discontinuous region.

modelled by a distance-corrected Morse potential, and the atom energy, which provides stabilisation/penalty for under-/over-coordinated atoms, remain smooth functions of distance.

The bond energy is a sum of three terms:  $\sigma$ ,  $\pi$ , and  $\pi\pi$  bond energies, each of which is an explicit function of a corresponding bond order. However, looking at the variation of the total bond order as a function of distance (Figure 1b), we see that this function is discontinuous with respect to distance. Similarly to the bond energy, the total bond order is a sum of the  $\sigma$ ,  $\pi$ , and  $\pi\pi$  contributions, which, in turn, depend on the bond distance. Thus, the energy and gradient terms, which depend on the total or partial bond orders either implicitly or explicitly, experience a discontinuity whenever the bond orders do. Obviously, such discontinuities in energies and forces will cause any gradient-based optimisation algorithm to fail.

In addition, numerical stability and, as a result, energy conservation during an MD simulation, are also compromised. Due to the finite time step size used in the integration of the equations of motion, the total energy has systematic fluctuations on a short time scale and a diffusive drift with an upward bias on a long time scale. Although both the fluctuations and the drift are acceptable if sufficiently small, unacceptably large drifts, can sometimes be obscured by large fluctuations until a significant part of the simulation has been performed. The resulting inaccuracy of such a simulation can produce unphysical behaviour and wasted computational resources.

We have determined that the origin of the poor energy conservation in ReaxFF is the use of several bond order and bond distance cutoffs. In each new configuration (or every time step), the various energy and force contributions are evaluated according to an updated bond order connectivity matrix. If a specific group (bond, angle, torsion or a hydrogen-bond) crossed the respective cutoff threshold, that group is discarded, and does not contribute to the respective energy/force contribution. Specifically, ReaxFF typically uses a bond order cutoff criterion of 0.001 for bonds, 0.0001 for valence angles and torsions, and 0.01 for a hydrogen-bond. In addition, it employs a distance based cutoff between a hydrogen atom and hydrogen-bond acceptor of 7.5 Å. The neglect of such small interactions affords a substantial

reduction in the memory and CPU time requirements, especially for large systems and long simulation times, which ReaxFF was designed to tackle. Since all cutoffs can be included as adjustable parameters during force field parameterisation, any errors that arise due to the neglect of some interactions are compensated for. Consequently, cutoffs must be considered an integral part of a force field. Apart from the bond order cutoff, all other valence cutoffs are not enclosed in the ReaxFF force field file, so great care should be taken when one uses published parameterisations with “default” values for all the remaining cutoffs, without thoroughly testing their effects.

To overcome the difficulties associated with bond order and bond distance cutoffs in the short-range terms in ReaxFF, one can choose to gradually lower the bond order cutoffs, and increase the donor-acceptor distance in hydrogen-bonded pairs. This solution seems to be the easiest in terms of implementation, and in fact, holds a key advantage: the various functional forms of ReaxFF are left intact, which guarantees a high level of transferability for the parameterised force field. However, at the same time, this solution results in a substantial increase in the memory and CPU time for all but the smallest systems. In addition, it does not cure the various discontinuities.

Another possible solution is to identify the potential functions that are especially sensitive to bond orders and have large gradients, and modify them accordingly, so that the change in the function value with respect to vanishing bond orders is significantly slower. Such a solution was recently attempted by Shchygol *et al.*,<sup>6</sup> where new functional forms were developed for the torsion and 4-body conjugation energy terms. The correction significantly reduced the discontinuity in the torsion angles, and allowed the authors to successfully minimise several challenging molecules.

To completely eliminate all the short-range discontinuities without counting negligibly weak interactions, we propose to use tapering functions to smoothly transition between bonded and non-bonded environments, while leaving regions outside the tapering range intact. Tapering functions are a popular choice in many simulation codes,<sup>46–48</sup> but differ

in their functional forms. Nevertheless, as demonstrated below, several conditions have to be strictly met, besides continuity of the tapering function itself, to avoid problems such as artificial minima, poor energy conservation, and numerical instabilities.

The minimal requirements for a tapering function,  $S(x)$ , are:

1. Smooth and monotonic decrease from 1 to 0 in a predefined tapering range,  $x_r$
2. Smooth 1<sup>st</sup> and 2<sup>nd</sup> derivatives
3. Vanishing derivatives at the limits of  $x_r$

The rationale for the above conditions is the following: the tapering function should interpolate between two limits of a discontinuous function,  $f(x)$ , where for one limit:  $f(x_{\max}) = f_{x_{\max}}$ , corresponding to a bonded environment, while at the other limit  $f(x_{\min}) = 0$ , i.e. a non-bonded environment. Condition 1 guarantees a smooth transition between the two limits, without introducing artificial stationary points. The numerical stabilities of geometry optimisation and integration algorithms generally depend on the smoothness of the 1<sup>st</sup> and 2<sup>nd</sup> derivatives.<sup>49</sup> Since  $S(x)$  is a constant outside the tapering range, its derivatives must be zero at the edges. Hence, conditions 2 and 3 must be met to ensure overall smoothness within and beyond the tapering range.

Although several functional forms have been previously suggested for a tapering function, we find that many of them fail to comply with conditions 2 and 3. A cosine taper<sup>50</sup> function with half a wavelength equal to  $x_r$ , and a cubic polynomial,<sup>51</sup> both have finite non-zero 2<sup>nd</sup> derivatives at the limits. The sine taper function<sup>52</sup> has finite non-zero 1<sup>st</sup> derivatives at the limits, which also violates conditions 2 and 3. The EAM taper function<sup>53</sup> has a finite non-zero 2<sup>nd</sup> derivative at one limit, again violating the required conditions. Damping functions, which are in broad use in empirical vdW corrections for density functional theory,<sup>54,55</sup> were designed to *asymptotically* approach the limit of zero damping, thus the 1<sup>st</sup> derivative does not have a compact support, violating condition 3.

The most general tapering function that satisfies all the above conditions is a 5<sup>th</sup> degree polynomial in bond order (or bond distance) between an atomic pair. Any higher degree polynomial can be used as well, with the advantage of a smoother transition region. A recent study has demonstrated that for a system of Lennard-Jones particles, and using a symplectic integrator, the total energy is well conserved for at least  $10^8$  time steps, provided that the potential and its first four derivatives are continuous.<sup>56</sup> This result originates from the existence of a slightly modified, *shadow Hamiltonian* ( $\tilde{H}$ ), for symplectic integrators, which the discrete trajectories follow.  $\tilde{H}$  is related to the original Hamiltonian,  $H$ , by an asymptotic expansion in time step size, and does not suffer from a long term energy drift due to a bounded error.<sup>57,58</sup> The existence of the first non-trivial term in the expansion requires that the potential and its first four derivatives are continuous, and it is only under this condition that the total energy remains constant for long periods of time.

ReaxFF employs a 7<sup>th</sup> degree polynomial to smoothly truncate the long-range Coulomb and vdW interactions<sup>14</sup> at the long tail boundary (typically  $x_{cut}=10$  to  $12 \text{ \AA}$ ). This long-range tapering begins at  $x = 0$  up to  $x = x_{cut}$  and ensures energy is conserved when charges move in and out of the cutoff boundary. Maintaining consistency with the ReaxFF long-range treatment, and to take advantage of better energy conservation during dynamic bond making and breaking processes, we propose a similar 7<sup>th</sup> degree polynomial to taper the short-range valence interactions [eqs. (1) and (2)]. The continuity of the polynomial ensures overall smoothness of the potential and its derivatives up to 3<sup>rd</sup> order at the cutoff boundaries (Supporting Information, Figure S1). Our choice establishes a compromise between good energy conservation and self-consistency on the one hand, and low computational overhead on the other hand:

$$S(x) = \begin{cases} 0, & \text{for } x \leq x_{\min} \\ Tap^{7\text{th}}(x), & \text{for } x_{\min} \leq x \leq x_{\max} \\ 1, & \text{for } x \geq x_{\max} \end{cases} \quad (1)$$

$$Tap^{7\text{th}}(x) = S_7 \times x^7 + S_6 \times x^6 + S_5 \times x^5 + S_4 \times x^4 + S_3 \times x^3 + S_2 \times x^2 + S_1 \times x^1 + 1 \quad (2)$$

where the  $S_i$  coefficients can be determined by conditions 1-3 above to obtain eq. (3):

$$\begin{aligned} S_1 &= 140/x_r^1, & S_2 &= -210/x_r^2, & S_3 &= 140/x_r^3, & S_4 &= -35/x_r^4, \\ S_5 &= 84/x_r^5, & S_6 &= -70/x_r^6, & S_7 &= 20/x_r^7, & x_r &= x_{\max} - x_{\min}. \end{aligned} \quad (3)$$

We note that another possible choice is the class of  $C^\infty$ -continuous transition functions,<sup>59</sup> one of which is presented in eq. (4):

$$S(x) = \frac{1}{1 + e^{x_r \times \left( \frac{1}{x - x_{\max}} + \frac{1}{x - x_{\min}} \right)}}. \quad (4)$$

As mentioned above, the ReaxFF architecture includes several different cutoffs for bond order and bond distance. Some of them, such as those employed for the long-range interactions and the total bond order, are specified in the force field parameters file (parameters 12, 13 and 30, respectively). For the valence and torsion angles, additional bond order cutoffs are set in the “control” file, which is a necessary run-time ingredient. Since each energy term, aside from long-range terms, is bond-order dependent, tapering the total bond order and individual  $\sigma$ ,  $\pi$ , and  $\pi\pi$  terms, removes the discontinuity from almost all valence energy terms, except for the hydrogen-bond term. Hydrogen-bonds are explicitly defined based on the bond order of the donor $\cdots$ hydrogen pair and the distance between the hydrogen $\cdots$ acceptor pair (the angle formed by the triplet of atoms participating in the hydrogen-bond is the third ingredient). Hence, in addition to tapering the bond order dependence, a separate tapering operation is needed to ensure continuity of the hydrogen $\cdots$ acceptor bond distance dependence.

Based on the 7<sup>th</sup> degree tapering polynomials for bond order and bond distance, we have derived new, minimally modified, functional forms for the various energy terms in ReaxFF,

with corresponding 1<sup>st</sup> derivatives. The tapered bond orders and energy contributions are presented in eqs. (5) to (12):

$$BO'_{ij} = S(BO'_{ij}{}^{\sigma}) \times BO'_{ij}{}^{\sigma} + S(BO'_{ij}{}^{\pi}) \times BO'_{ij}{}^{\pi} + S(BO'_{ij}{}^{\pi\pi}) \times BO'_{ij}{}^{\pi\pi} \quad (5)$$

$$E_{\text{bond}} = E_{\text{bond}} \quad (6)$$

$$E_{\text{val}} = E_{\text{val}} \times S(BO_{ij}) \times S(BO_{ik}) \quad (7)$$

$$E_{\text{pen}} = E_{\text{pen}} \times S(BO_{ij}) \times S(BO_{ik}) \quad (8)$$

$$E_{\text{coa}} = E_{\text{coa}} \times S(BO_{ij}) \times S(BO_{ik}) \quad (9)$$

$$E_{\text{hbond}} = E_{\text{hbond}} \times S(BO_{ij}) \times S(r_{ik}) \quad (10)$$

$$E_{\text{tors}} = E_{\text{tors}} \times S(BO_{ij}) \times S(BO_{ik}) \cdot S(BO_{jl}) \quad (11)$$

$$E_{\text{conj}} = E_{\text{conj}} \times S(BO_{ij}) \times S(BO_{ik}) \cdot S(BO_{jl}) \quad (12)$$

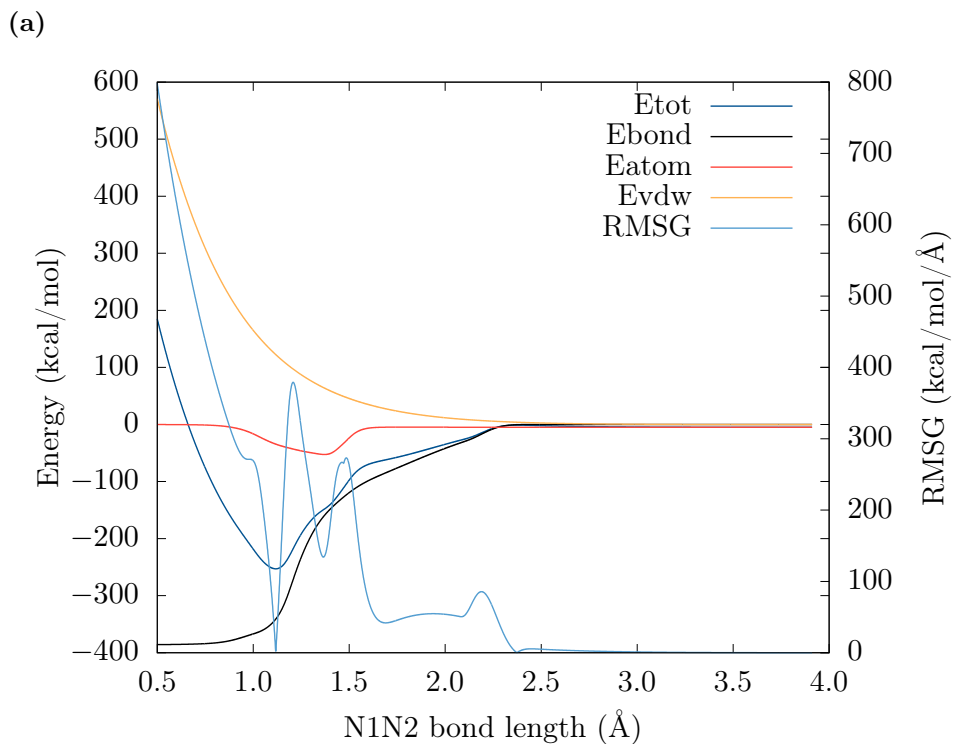
We note that the bond orders that appear in eq. (5) are corrected for over- and under-coordination before any of the valence energy contributions, eqs. (7) to (12), are calculated. Also, note that the expression for bond energy,  $E_{\text{bond}}$ , does not require additional tapering beyond the bond order tapering that is performed for the bond orders [eq. (5)]. This is because all the other terms have specific cutoffs in addition to the bond order cutoffs.

Besides the bond order, valence angle, torsion angle, and hydrogen-bond cutoffs, ReaxFF uses additional, hard-coded, cutoffs that might lead to energy discontinuities. These are powers (squared and cubed) of the valence and torsion angles cutoffs, which are used to further reduce the number of pairs and triples of atoms. In addition, a third layer of truncation is employed on the *corrected* bond orders, where the  $\sigma$ ,  $\pi$  and  $\pi\pi$  bond orders are set to zero, if their value falls below  $10^{-10}$ . Although this is apparently a small threshold, we find that it also leads to energy discontinuities. Hence, all the aforementioned hard-coded cutoffs were completely disabled in this study. For the bond order and bond distance cutoffs, we have chosen a tapering range of  $x_r = x_{\text{max}} - x_{\text{min}} = 3x_{\text{min}}$  and  $0.9x_{\text{max}}$ , respectively, where the

values for  $x_{\min}$  and  $x_{\max}$  were specified above.

We now analyse the performance of the newly formulated, tapered ReaxFF, first returning to the simple benchmark system of molecular  $N_2$ . As is clear from Figure 2a, the discontinuity in the RMSG disappears and all energy terms are now continuous. All the energy curves remain nearly identical to the original ones due to the limited tapering range. This result is encouraging since it suggests that no reparameterisation of available force fields will be required for the new formulation. However, at the same time, the tapering transition introduces a bump in the RMSG curve, which manifests itself as an artificial force during dynamics. We note, however, that this result and the previous bond compression/expansion curves for  $N_2$  were generated with a cutoff larger by 3 orders of magnitude compared to the optimised value in order to highlight the problem. For typical cutoffs, the artificial force that is produced by the tapering polynomial is significantly reduced, and does not have any noticeable effect. All the other benchmark systems used the typical values for every cutoff, and the resulting structures successfully converged to local minima with vanishing forces. Figure 2b presents a comparison of the final structure of trpzip2 peptide for the tapered ReaxFF and the original formulation. The original structure deviates significantly from the true local minimum, and is the result of an unsuccessful optimisation. The RMSD between the structures is  $1.479\text{\AA}$ , indicating that the final structure obtained with original ReaxFF is far from a local minimum. The trpzip2 structure serves as a useful benchmark problem for optimisation because of the relatively large number of degrees of freedom, and the soft modes, including both torsional and hydrogen bonded interactions. For the tapered ReaxFF, however, there is no problem and the L-BFGS algorithm smoothly converges to a local minimum.

Usually, slight deviations from the optimised structure do not have any direct effect on subsequent dynamics, and geometry optimisation is mainly used in MD simulations to avoid initial steric clashes between atoms. Hence, provided that the system starts not too far from a nearby local minimum, and the temperature in the subsequent dynamics stage is



(b)

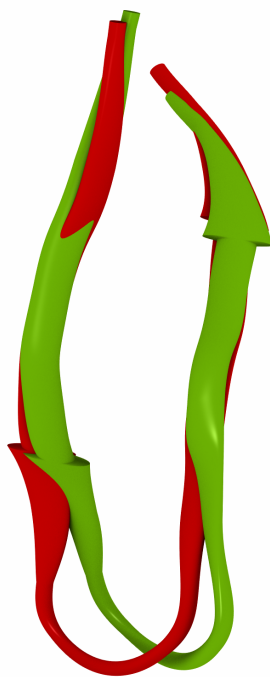


**Figure 2.** Performance of Tapered ReaxFF for benchmark systems. (a) Two body energy curves and RMSG for molecular  $N_2$ . (b) trpzip2 peptide structures after geometry optimisation. Red: original ReaxFF, Green: tapered ReaxFF. Ribbon representation for an antiparallel  $\beta$  hairpin prepared using VMD.<sup>60</sup>

not too high compared with the surrounding barriers, the dynamics will not be dramatically affected. On the other hand, if the system starts in a region where relevant barriers are comparable to  $kT$ , the system might jump out of the catchment basin to a distant state, and subsequent dynamics could be severely affected. Moreover, if the initial forces are large, energy conservation could potentially be violated if the time step size is not small enough.

To compare the two formulations, original ReaxFF and tapered ReaxFF, with respect to dynamics, we have performed a set of MD simulations on four systems: trpzip2 peptide, a single crystal of TNT, bulk liquid water and a single crystal of Benzene. These systems constitute several challenging cases. Liquid water and biomolecules, such as the trpzip2 peptide, are usually simulated at room temperature, and such systems are particularly prone to being trapped in intermediate states for prolonged periods of time. On the other hand, simulations crystalline materials are challenging because they are periodic systems, with both molecular and crystalline degrees of freedom. In addition, the decomposition of energetic materials, such as TNT, results in highly exothermic reactions, which leads to additional heating and very rich chemistry.<sup>27</sup> Thus, decomposition mechanisms and the corresponding kinetics could be significantly affected by poor energy conservation.

For the peptide, thermalisation and equilibration runs were conducted at room temperature prior to a production run in the NVE ensemble. Thermalisation was achieved by heating the system to 300 K during 10 ps using a Berendsen thermostat with a coupling constant of 25 fs. Then, a further constant temperature equilibration at 300 K was carried out for 50 ps. In the final stage, the system was evolved in the NVE ensemble for another 50 ps, and we then compare key thermodynamic and structural features between the two ReaxFF formulations. For the water system, heating to 300 K during 10 ps and thermalisation at 300 K for additional 10 ps were carried out before a pressure equilibration stage (300 K, 1 atm) which lasted 50 ps. At this point, NVE simulation was started for additional 50 ps. The time step size during all stages was set to 0.25 fs, which reflects a conservative choice.

For the case of TNT crystal, a standard “cookoff” procedure<sup>24</sup> was simulated, where an

ultrashort (1 ps) heating (to 4500 K) stage on a geometry optimised and pre-equilibrated crystal (300 K, 1 atm) was followed by an NVE stage for 20 ps. The time step size used in these stages was 0.05 fs. For Benzene, the system was heated to 218 K during 10 ps. Thereafter, a thermalisation stage (10 ps) followed before commencing the final stage of NVE dynamics for another 20 ps. For these low temperature calculations, the time step size was 0.25 fs.

We begin with the analysis of the trpzip2 peptide system. The resulting temperature evolution for both formulations was very similar (Supporting Information, Figure S2), suggesting that possible artificial forces in the tapering region did not cause any system heating. The radial pair distribution function was calculated based on the carbon backbone and displayed identical patterns for the two structures (Supporting Information, Figure S3). This result further supports the validity of our implementation, and demonstrates that both the short- and long-range order in the system remain intact. However, a rather surprising discrepancy was observed in the all-atom RMSD plots (Supporting Information, Figure S4), in which the initial structures at  $t = 0$  served as a reference. According to these results, the trpzip2 peptide in the original ReaxFF is “softer”, with up to 40% larger RMSD values. Although differences in RMSD plots are traditionally attributed to the presence of artificial forces (or minima) that tend to restrict the motion of the covalent framework,<sup>51,61,62</sup> our results do not support this proposition. A careful analysis and visualisation of the structure, revealed that the original ReaxFF led to dissociation of an ammonia molecule at the very beginning of the heating stage. Clearly, this dissociated state might imply a force field artefact, however it highlights an important and commonly overlooked role for geometry optimisation: not only to avoid steric clashes but also to produce more stable dynamics. In this case, the original ReaxFF potential could not be converged to a local minimum, but produced a high-energy structure, which resulted in unphysical dissociation at 300K. On the other hand, several independent tapered ReaxFF simulations did not exhibit this behaviour.

The densities of the TNT single crystal following the NPT simulation stage were 1.59

and  $1.69 \text{ g/cm}^3$  for the original and tapered ReaxFF, respectively. Both values are in good agreement with the experimental density at room temperature ( $1.65 \text{ g/cm}^3$ ) and we note that no (artificial) dissociation occurred during the equilibration stages. Since it is known that the thermal decomposition of many organic high explosives is pressure and density-dependent,<sup>26,27</sup> we have used the equilibrated configuration of the tapered formulation as the starting point for the “cookoff” stage with both formulations. This choice provides a fair comparison, so any differences between the two simulations should be primarily attributed to the discontinuous energies and forces.

The water system exhibited a similar behaviour in both formulations during the heating and equilibration steps. Specifically, the obtained density at the end of the pressure equilibration stage was  $1.01 \text{ g/cm}^3$  for both formulations, in excellent agreement with the experimental density at STP conditions of  $0.99 \text{ g/cm}^3$ . The radial pair distribution function between Oxygen atoms during NVE dynamics was very much similar in both formulations (Supporting Information, Figure S5). For the case of the crystalline Benzene system, no difference was observed between the formulations during the heating and thermalisation stages. These findings further substantiate the validity of our approach and suggest a broad transferability.

Arguably, the most important comparison between the two formulations is the total energy evolution in the system during NVE dynamics. Poor energy conservation leads to deviation from Hamiltonian dynamics, and thus results in unphysical behaviour. Therefore, methods that fail to conserve the energy of closed systems should be avoided, regardless of whether they are used in simulations for NVE or other ensembles. Continuous coupling to a heat bath only masks the inherent problem, and prohibits accurate simulations of observables that are sensitive to energy propagation.

Figure 3 presents the total energies of the trpzip2 peptide, TNT single crystal, bulk water and Benzene crystal systems for the original and tapered ReaxFF formulations. The tapering of the valence interactions leads to a dramatic improvement in energy conservation for all

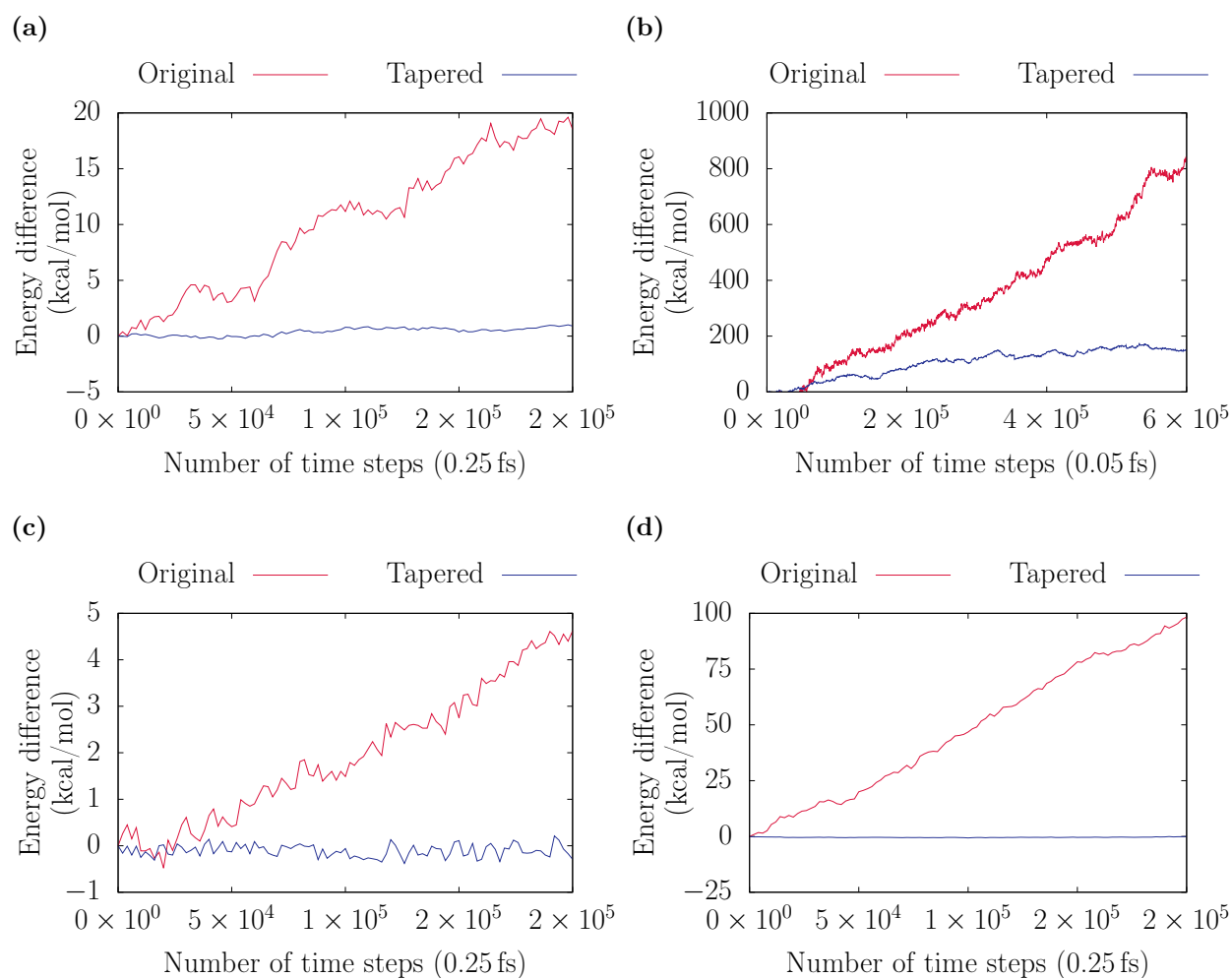


**Figure 3.** Total energy conservation during NVE dynamics for original (red line) and tapered (blue line) ReaxFF. (a) Trpzip2 peptide; (b) TNT single crystal; (c) Liquid water; (d) Benzene single crystal

systems. Three general observations are worth mentioning: (a) the fluctuations around the mean total energy in the original ReaxFF implementation are substantially larger; (b) the mean total energy in the original ReaxFF implementation rises steadily. Whereas the former problem is related to the discrepancy between the discrete and analytic Hamiltonians due to roundoff errors,<sup>56</sup> the latter effect is a systematic error that originates from the discontinuities in the potential and its derivatives in the *shadow Hamiltonian*. In the tapered case, the total energies remain bounded in the long time limit; and (c) the total energy in the case of the TNT system with a tapered ReaxFF formulation exhibits a somewhat small but still noticeable increase. Considering the very high temperature of the system ( $>5000$  K), this effect may result from the finite time step, or from the relatively short neighbour list distance (5 Å), or from a neighbour list update interval that is too short (every 25 time steps), which is the ReaxFF default.

Analysis of the energy conservation and drift rate reveals a dramatic improvement for the new tapered formulation (Table 2). We used a linear fit to calculate the drift rate from the last 20 ps, while the degree of energy conservation was calculated from the difference between final and initial energies relative to the initial total energy. For trpzip2, the original formulation gains on average 0.41 kcal/mol every 1 ps, which yields an energy conservation of 0.08% over 50 ps. We can extrapolate to the 1 ns time limit (assuming a linear drift), to obtain a gross estimate of the energy conservation for a more realistic time scale in modern all-atom MD simulations. This extrapolation results in energy conservation of 1.6% and is probably a lower limit. In the case of the TNT system, the original formulation gains almost 30 kcal/mol every 1 ps, which amounts to a substantial violation of energy conservation (3.57%) during this relatively short simulation. For the liquid water and the Benzene crystal systems, one can notice a substantial improvement in the conservation of the total energy. By extrapolation of the original ReaxFF values to a 1 ns limit, these systems exhibit total energy violations of 2% and 41%, respectively. Remarkably, the tapered formulation results in no noticeable change in the total energy of these systems, as is expected from a symplectic

integrator.

Another standard measure of simulation accuracy, besides long term energy conservation, is the ratio of the fluctuations in total energy,  $\langle \Delta E^2 \rangle^{1/2}$ , to the fluctuations in the kinetic energy of the system,  $\langle \Delta KE^2 \rangle^{1/2}$ . Typical values that are considered acceptable for this quantity are  $< 10\%$ .<sup>61,63</sup> Table 2 shows that the tapered formulation achieves good accuracy in both systems, while the original ReaxFF is less reliable.

A detailed analysis of the temperature evolution and final stable products at the end of the TNT NVE simulation revealed that the original formulation leads to a constant heating, ultimately reaching temperatures of almost 7000 K, before severe numerical instabilities halted the run. The final state of the system consisted of mainly evaporated atoms. For the tapered ReaxFF a steady state temperature of 5500 K was maintained, and several thermodynamically stable detonation products were observed ( $N_2$ ,  $H_2O$ ,  $CO$ ,  $H_2$  and soot). All other systems exhibited similar reactivity for the two formulations due to the low system temperatures, except for the minor dissociation of trpzip2 peptide during the initial heating stage.

**Table 2: Total energy drift rate ( $\text{kcal mol}^{-1} \text{ps}^{-1}$ ), energy conservation (%), and ratio of square root of the fluctuations in total energy to fluctuations in kinetic energy (%) for two systems using the original (O) and tapered (T) ReaxFF formulations**

ReaxFF	trpzip2		TNT crystal		liquid water		Benzene crystal	
Formulation	O	T	O	T	O	T	O	T
Drift rate	0.41	0.02	27.86	1.01	0.10	0.00	2.04	0.00
Energy conservation	0.08	0.003	3.57	0.51	0.01	0.00	0.23	0.00
$(\langle \Delta E^2 \rangle / \langle \Delta KE^2 \rangle)^{1/2}$	68.87	3.69	74.72	4.86	14.12	1.21	152.48	1.28

At this stage, we would like to comment on the choice of the tapering range for the short-range bond order and distance cutoffs in tapered ReaxFF. From Figure 1a, we note that rather high artificial forces can be introduced if the discontinuity is large compared to the tapering range. Indeed, it was shown that for long-range Coulomb interactions, even with standard cutoffs (10-12Å), these forces could lead to significant distortions of the structure,

in addition to the appearance of artificial minima on the potential energy surface.<sup>51,62</sup> Using large tapering ranges successfully mitigates this problem, which is not too severe for the valence terms, compared to electrostatic interactions. To estimate the sensitivity of the force field to the tapering range, we have repeated the calculations for the  $N_2$  molecule using the same exaggerated bond order cutoff for different tapering ranges, as shown in Figure 4.

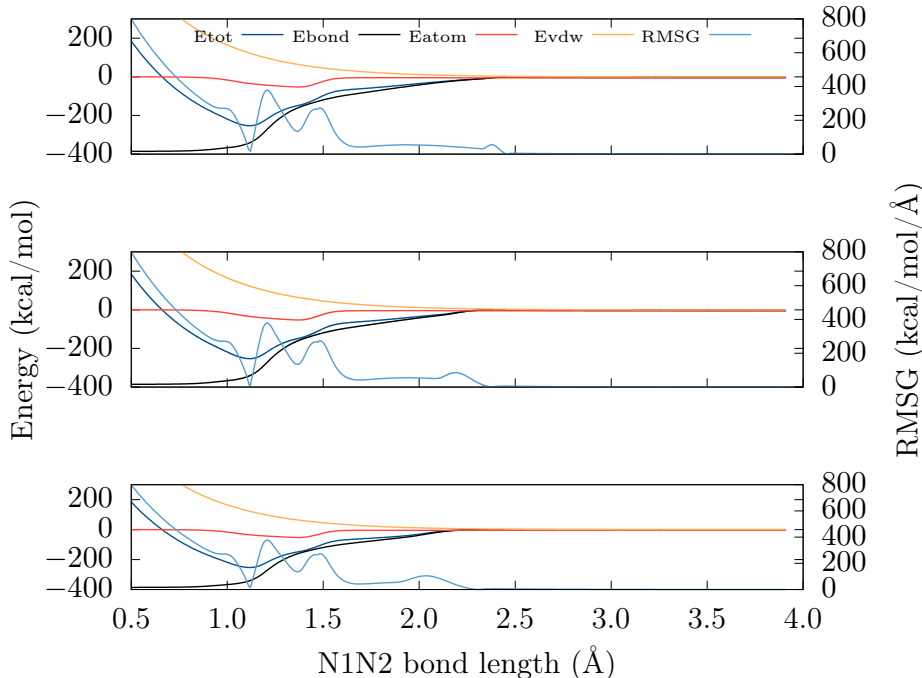


**Figure 4.** Effect of tapering range,  $x_r = x_{\max} - x_{\min}$ , on the potential energy terms and RMSG of molecular  $N_2$ . Top panel:  $x_{\max} = 2x_{\min}$ , Middle panel:  $x_{\max} = 4x_{\min}$ , Bottom panel:  $x_{\max} = 6x_{\min}$

We infer from Figure 4 that the potential energy terms and the RMSG are rather insensitive to the particular tapering range within reasonable bounds. In all the examples, no artificial minima were introduced, although there are some artificial forces in the tapering range. However, this example uses a bond order cutoff exaggerated by 3 orders of magnitude. Using typical bond order cutoffs results in no artificial forces whatsoever, even for the relatively narrow tapering range of  $x_{\max} = 2x_{\min}$ .

If, for any particular system, the tapering range leads to somewhat large changes to the potential, the respective force field can be easily reparameterised. With a slight adjustment of

the force field parameters, any differences between ReaxFF and the target *ab initio* potential energy surface will be minimised. In the current study, such reparameterisation was found to be unnecessary.

To further validate the transferability of our approach, we have compared the predicted energies for a large set of organic materials between tapered and original ReaxFF formulations with respect to DFT calculations (calculated at the B3LYP/6-31G(d) level or better). The dataset is composed of energy differences for various bond compression and expansion curves, valence and torsion angle bending, heats of formation, sublimation energies and reaction barriers. It includes both molecules and crystal phases of common high-energy materials, overall resulting in over 1600 equilibrated species and 40 reaction pathways<sup>64</sup> (Figure 5).

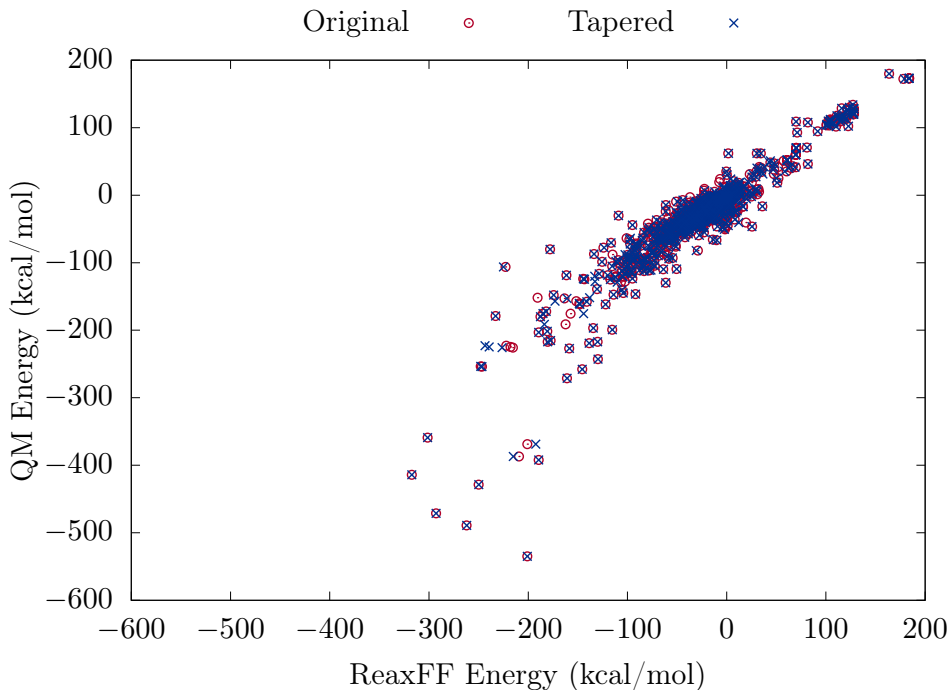


**Figure 5.** Performance of tapered and original ReaxFF on a dataset of high-energy materials with respect to QM energies from DFT calculations

We make two key observations regarding the comparison presented in Figure 5. Firstly, the performance of the original ReaxFF force field<sup>27</sup> is very impressive, showing minor deviations in the high-energy, statistically unlikely, structures, where high accuracy is usually sacrificed in favour of more stable structures during parameterisation. Secondly, the tapered

formulation has an almost identical performance in terms of both accuracy and precision, compared to the original formulation. These results further validate our approach and implementation, and suggest that the same formulation can be used with existing parameters for published force fields. We also note that the tapering scheme does not have any significant computational overheads in a typical ReaxFF simulation. This is because the most time consuming stage in ReaxFF MD is the iterative solution of the partial charges, which do not depend on bond orders. Moreover, the scheme is compatible with all major simulation codes, including LAMMPS,<sup>65</sup> PuReMD<sup>66</sup> and GULP.<sup>48</sup>

The numerical smoothness and orders of magnitude increase in simulation accuracy (at no additional cost) will facilitate exciting new applications for ReaxFF force fields, such as accurate all-atom simulations of biomolecular chemistry for unprecedented time scales.

## Acknowledgement

D. F. is grateful to A. C. T. van Duin, T. Verstraelen and J. Gale for fruitful discussions. D. F. acknowledges generous support from the Herchel Smith Post-Doctoral Research Fellowship at the University of Cambridge.

The authors declare no competing financial interest.

## References

- (1) Pauling, L. Atomic Radii and Interatomic Distances in Metals. *J. Am. Chem. Soc.* **1947**, *69*, 542–553.
- (2) Mortier, W. J.; Ghosh, S. K.; Shankar, S. Electronegativity-equalization method for the calculation of atomic charges in molecules. *J. Am. Chem. Soc.* **1986**, *108*, 4315–4320.
- (3) Rappe, A. K.; Goddard, W. A. Charge equilibration for molecular dynamics simulations. *J. Phys. Chem.* **1991**, *95*, 3358–3363.

- (4) Verstraelen, T.; Ayers, P. W.; Van Speybroeck, V.; Waroquier, M. ACKS2: Atom-condensed Kohn-Sham DFT approximated to second order. *J. Chem. Phys.* **2013**, *138*, 074108.
- (5) Furman, D.; Carmeli, B.; Zeiri, Y.; Kosloff, R. Enhanced Particle Swarm Optimization Algorithm: Efficient Training of ReaxFF Reactive Force Fields. *J. Chem. Theory Comput.* **2018**, *14*, 3100–3112.
- (6) Shchygol, G.; Yakovlev, A.; Trnka, T.; C.T. van Duin, A.; Verstraelen, T. ReaxFF Parameter Optimization with Monte Carlo and Evolutionary Algorithms: Guidelines and Insights. *ChemRxiv* **2019**,
- (7) Mishra, A.; Hong, S.; Rajak, P.; Sheng, C.; Nomura, K.-i.; Kalia, R. K.; Nakano, A.; Vashishta, P. Multiobjective genetic training and uncertainty quantification of reactive force fields. *npj Comput. Mater.* **2018**, *4*, 42.
- (8) Jaramillo-Botero, A.; Naserifar, S.; Goddard, W. A. General Multiobjective Force Field Optimization Framework, with Application to Reactive Force Fields for Silicon Carbide. *J. Chem. Theory Comput.* **2014**, *10*, 1426–1439.
- (9) Dittner, M.; Müller, J.; Aktulga, H. M.; Hartke, B. Efficient global optimization of reactive force-field parameters. *J. Comp. Chem.* **2015**, *36*, 1550–1561.
- (10) Qian, H. J.; Van Duin, A. C. T.; Morokuma, K.; Irle, S. Reactive molecular dynamics simulation of fullerene combustion synthesis: ReaxFF vs DFTB potentials. *J. Chem. Theory Comput.* **2011**, *7*, 2040–2048.
- (11) Boes, J. R.; Groenenboom, M. C.; Keith, J. A.; Kitchin, J. R. Neural network and ReaxFF comparison for Au properties. *Int. J. Quantum Chem.* **2016**, *116*, 979–987.
- (12) Ashraf, C.; Jain, A.; Xuan, Y.; van Duin, A. C. T. ReaxFF based molecular dynamics

- simulations of ignition front propagation in hydrocarbon/oxygen mixtures under high temperature and pressure conditions. *Phys. Chem. Chem. Phys.* **2017**, *19*, 5004–5017.
- (13) Ashraf, C.; van Duin, A. C. Extension of the ReaxFF Combustion Force Field toward Syngas Combustion and Initial Oxidation Kinetics. *J. Phys. Chem. A* **2017**, *121*, 1051–1068.
- (14) Chenoweth, K.; van Duin, A. C. T.; Goddard III, W. A. ReaxFF Reactive Force Field for Molecular Dynamics Simulations of Hydrocarbon Oxidation. *J. Phys. Chem. A* **2008**, *112*, 1040–1053.
- (15) Monti, S.; Srifa, P.; Kumaniaev, I.; Samec, J. S. M. ReaxFF Simulations of Lignin Fragmentation on a Palladium-Based Heterogeneous Catalyst in Methanol/Water Solution. *J. Phys. Chem. Lett.* **2018**, *9*, 5233–5239.
- (16) Senftle, T. P.; van Duin, A. C.; Janik, M. J. Determining in situ phases of a nanoparticle catalyst via grand canonical Monte Carlo simulations with the ReaxFF potential. *Catal. Commun.* **2014**, *52*, 72–77.
- (17) Chaban, V. V.; Prezhdo, O. V. Haber Process Made Efficient by Hydroxylated Graphene: Ab Initio Thermochemistry and Reactive Molecular Dynamics. *J. Phys. Chem. Lett.* **2016**, *7*, 2622–2626.
- (18) Hong, S.; Krishnamoorthy, A.; Rajak, P.; Tiwari, S.; Misawa, M.; Shimojo, F.; Kalia, R. K.; Nakano, A.; Vashishta, P. Computational Synthesis of MoS<sub>2</sub> Layers by Reactive Molecular Dynamics Simulations: Initial Sulfidation of MoO<sub>3</sub> Surfaces. *Nano Lett.* **2017**, *17*, 4866–4872.
- (19) Monti, S.; Jose, J.; Sahajan, A.; Kalarikkal, N.; Thomas, S. Structure and dynamics of gold nanoparticles decorated with chitosan/gentamicin conjugates: ReaxFF molecular dynamics simulations to disclose drug delivery. *Phys. Chem. Chem. Phys.* **2019**, *21*, 13099–13108.

- (20) Chaban, V. V.; Pal, S.; Prezhdo, O. V. Laser-Induced Explosion of Nitrated Carbon Nanotubes: Nonadiabatic and Reactive Molecular Dynamics Simulations. *J. Am. Chem. Soc.* **2016**, *138*, 15927–15934.
- (21) Chaban, V. V.; Fileti, E. E.; Prezhdo, O. V. Buckybomb: Reactive Molecular Dynamics Simulation. *J. Phys. Chem. Lett.* **2015**, *6*, 913–917.
- (22) Onofrio, N.; Guzman, D.; Strachan, A. The dynamics of copper intercalated molybdenum ditelluride. *J. Chem. Phys.* **2016**, *145*, 194702.
- (23) Trnka, T.; Tvaroška, I.; Koča, J. Automated Training of ReaxFF Reactive Force Fields for Energetics of Enzymatic Reactions. *J. Chem. Theory Comput.* **2018**, *14*, 291–302.
- (24) van Duin, A. C. T.; Zeiri, Y.; Dubnikova, F.; Kosloff, R.; Goddard III, W. A. Atomistic-Scale Simulations of the Initial Chemical Events in the Thermal Initiation of Triacetoneperoxide. *J. Am. Chem. Soc.* **2005**, *127*, 11053–11062.
- (25) Budzien, J.; Thompson, A. P.; Zybin, S. V. Reactive Molecular Dynamics Simulations of Shock Through a Single Crystal of Pentaerythritol Tetranitrate. *J. Phys. Chem. B* **2009**, *113*, 13142–13151.
- (26) Rom, N.; Zybin, S. V.; van Duin, A. C. T.; Goddard, W. A.; Zeiri, Y.; Katz, G.; Kosloff, R. Density-Dependent Liquid Nitromethane Decomposition: Molecular Dynamics Simulations Based on ReaxFF. *J. Phys. Chem. A* **2011**, *115*, 10181–10202.
- (27) Furman, D.; Kosloff, R.; Dubnikova, F.; Zybin, S. V.; Goddard, W. A.; Rom, N.; Hirschberg, B.; Zeiri, Y. Decomposition of Condensed Phase Energetic Materials: Interplay between Uni- and Bimolecular Mechanisms. *J. Am. Chem. Soc.* **2014**, *136*, 4192–4200.
- (28) Islam, M. M.; Strachan, A. Reactive Molecular Dynamics Simulations to Investigate the Shock Response of Liquid Nitromethane. *J. Phys. Chem. C* **2019**, *123*, 2613–2626.

- (29) Furman, D.; Kosloff, R.; Zeiri, Y. Effects of nanoscale heterogeneities on the reactivity of shocked erythritol tetranitrate. *J. Phys. Chem. C* **2016**, *120*, 28886–28893.
- (30) Furman, D.; Dubnikova, F.; Van Duin, A.; Zeiri, Y.; Kosloff, R. Reactive Force Field for Liquid Hydrazoic Acid with Applications to Detonation Chemistry. *J. Phys. Chem. C* **2016**, *120*.
- (31) Oxley, J.; Furman, D.; Brown, A.; Dubnikova, F.; Smith, J.; Kosloff, R.; Zeiri, Y. Thermal Decomposition of Erythritol Tetranitrate: A Joint Experimental and Computational Study. *J. Phys. Chem. C* **2017**, *121*.
- (32) Furman, D.; Kosloff, R.; Zeiri, Y. Mechanism of Intact Adsorbed Molecules Ejection Using High Intensity Laser Pulses. *J. Phys. Chem. C* **2016**, *120*, 11306–11312.
- (33) Kalson, N.-H.; Furman, D.; Zeiri, Y. Cavitation-Induced Synthesis of Biogenic Molecules on Primordial Earth. *ACS Cent. Sci.* **2017**, *3*, 1041–1049.
- (34) Zhang, W.; van Duin, A. C. T. Second-Generation ReaxFF Water Force Field: Improvements in the Description of Water Density and OH-Anion Diffusion. *J. Phys. Chem. B* **2017**, *121*, 6021–6032.
- (35) Gale, J. D.; Raiteri, P.; van Duin, A. C. T. A reactive force field for aqueous-calcium carbonate systems. *Phys. Chem. Chem. Phys.* **2011**, *13*, 16666.
- (36) Rahaman, O.; van Duin, A. C. T.; Bryantsev, V. S.; Mueller, J. E.; Solares, S. D.; Goddard, W. A.; Doren, D. J. Development of a ReaxFF Reactive Force Field for Aqueous Chloride and Copper Chloride. *J. Phys. Chem. A* **2010**, *114*, 3556–3568.
- (37) Wales, D. J. *Energy landscapes*; Cambridge University Press, 2003; p 681.
- (38) Wales, D. J. Exploring Energy Landscapes. *Annu. Rev. Phys. Chem.* **2018**, *69*, 401–425.
- (39) Wales, D. J. A microscopic basis for the global appearance of energy landscapes. *Science* **2001**, *293*, 2067–70.

- (40) Asenjo, D.; Stevenson, J. D.; Wales, D. J.; Frenkel, D. Visualizing Basins of Attraction for Different Minimization Algorithms. *J. Phys. Chem. B* **2013**, *117*, 12717–12723.
- (41) Lewis, A. S.; Overton, M. L. Nonsmooth optimization via quasi-Newton methods. *Math. Program.* **2013**, *141*, 135–163.
- (42) Byrd, R. H.; Lu, P.; Nocedal, J.; Zhu, C. A Limited Memory Algorithm for Bound Constrained Optimization. *Siam. J. Sci. Comput.* **1995**, *16*, 1190–1208.
- (43) Monti, S.; Corozzi, A.; Fristrup, P.; Joshi, K. L.; Shin, Y. K.; Oelschlaeger, P.; van Duin, A. C. T.; Barone, V. Exploring the conformational and reactive dynamics of biomolecules in solution using an extended version of the glycine reactive force field. *Phys. Chem. Chem. Phys.* **2013**, *15*, 15062.
- (44) Goverapet Srinivasan, S.; Van Duin, A. C. T.; Ganesh, P. Development of a ReaxFF potential for carbon condensed phases and its application to the thermal fragmentation of a large fullerene. *J. Phys. Chem. A* **2015**, *119*, 571–580.
- (45) Mao, Q.; Ren, Y.; Luo, K. H.; van Duin, A. C. T. Dynamics and kinetics of reversible homo-molecular dimerization of polycyclic aromatic hydrocarbons. *The Journal of Chemical Physics* **2017**, *147*, 244305.
- (46) Case, D. A.; Cheatham, T. E.; Darden, T.; Gohlke, H.; Luo, R.; Merz, K. M.; Onufriev, A.; Simmerling, C.; Wang, B.; Woods, R. J. The Amber biomolecular simulation programs. *J. Comp. Chem.* **2005**, *26*, 1668–1688.
- (47) Brooks, B. R.; Brooks, C. L.; Mackerell, A. D.; Nilsson, L.; Petrella, R. J.; Roux, B.; Won, Y.; Archontis, G.; Bartels, C.; Boresch, S.; Caffisch, A.; Caves, L.; Cui, Q.; Dinner, A. R.; Feig, M.; Fischer, S.; Gao, J.; Hodoscek, M.; Im, W.; Kuczera, K.; Lazaridis, T.; Ma, J.; Ovchinnikov, V.; Paci, E.; Pastor, R. W.; Post, C. B.; Pu, J. Z.; Schaefer, M.; Tidor, B.; Venable, R. M.; Woodcock, H. L.; Wu, X.; Yang, W.;

- York, D. M.; Karplus, M.; York, D.; Karplus, M. CHARMM: the biomolecular simulation program. *J. Comp. Chem.* **2009**, *30*, 1545–614.
- (48) Gale, J. D.; Rohl, A. L. The General Utility Lattice Program ( GULP ). *Mol. Simulat.* **2003**, *29*, 291–341.
- (49) Zhou, X. W.; Jones, R. E. Effects of cutoff functions of Tersoff potentials on molecular dynamics simulations of thermal transport. *Model. Simul. Mater. Sci. Eng* **2011**, *19*, 025004.
- (50) Jiang, Z.; Brown, R. Modelling oxygen defects in silicon crystals using an empirical interatomic potential. *Chem. Eng. Sci.* **1994**, *49*, 2991–3000.
- (51) Steinbach, P. J.; Brooks, B. R. New sphericalcutoff methods for longrange forces in macromolecular simulation. *J. Comp. Chem.* **1994**, *15*, 667–683.
- (52) Watanabe, T.; Fujiwara, H.; Noguchi, H.; Hoshino, T.; Ohdomari, I. Novel Interatomic Potential Energy Function for Si, O Mixed Systems. *Jpn. J. Appl. Phys.* **1999**, *38*, L366–L369.
- (53) Baskes, M. Determination of modified embedded atom method parameters for nickel. *Mater. Chem. Phys.* **1997**, *50*, 152–158.
- (54) Tang, K. T.; Peter Toennies, J. An improved simple model for the van der Waals potential based on universal damping functions for the dispersion coefficients. *J. Chem. Phys.* **1984**, *80*, 3726–3741.
- (55) Liu, Y.; Goddard, W. A. A universal damping function for empirical dispersion correction on density functional theory. *Mater. Trans.* **2009**, *50*, 1664–1670.
- (56) Toxvaerd, S.; Heilmann, O. J.; Dyre, J. C. Energy conservation in molecular dynamics simulations of classical systems. *J. Chem. Phys.* **2012**, *136*, 224106.

- (57) Hairer, E. Backward analysis of numerical integrators and symplectic methods. *Ann. Numer. Math.* **1994**, *1*, 107–132.
- (58) Yoshida, N. Symplectic Integrators for Hamiltonian Systems: Basic Theory. *SIAU* **1992**, 407–411.
- (59) Schutz, B. F. *Geometrical methods of mathematical physics*; Cambridge University Press, 1980; p 250.
- (60) Humphrey, W.; Dalke, A.; Schulten, K. VMD – Visual Molecular Dynamics. *J. Mol. Graph.* **1996**, *14*, 33–38.
- (61) Kitchen, D. B.; Hirata, F.; Westbrook, J. D.; Levy, R.; Kofke, D.; Yarmush, M. Conserving energy during molecular dynamics simulations of water, proteins, and proteins in water. *J. Comp. Chem.* **1990**, *11*, 1169–1180.
- (62) Norberg, J.; Nilsson, L. On the truncation of long-range electrostatic interactions in DNA. *Biophys. J.* **2000**, *79*, 1537–1553.
- (63) Berendsen, H. J. C.; Gunsteren, W. F. *Molecular Liquids*; Springer Netherlands: Dordrecht, 1984; pp 475–500.
- (64) Strachan, A.; van Duin, A. C. T.; Chakraborty, D.; Dasgupta, S.; Goddard, W. A. Shock Waves in High-Energy Materials: The Initial Chemical Events in Nitramine RDX. *Phys. Rev. Lett.* **2003**, *91*, 098301.
- (65) Plimpton, S. Fast Parallel Algorithms for Short-Range Molecular Dynamics. *J. Comp. Phys.* **1995**, *117*, 1 – 19.
- (66) Kylasa, S.; Aktulga, H.; Grama, A. PuReMD-GPU: A reactive molecular dynamics simulation package for GPUs. *J. Comp. Phys.* **2014**, *272*, 343 – 359.

## Supporting Information Available

7<sup>th</sup> degree tapering polynomial and higher derivatives, evolution of temperature for trpzip2 peptide, radial pair distribution function of carbon atoms for trpzip2 peptide, all-atom RMSD for trpzip2 peptide, radial pair distribution function for oxygen atoms in bulk liquid water. This material is available free of charge via the Internet at <http://pubs.acs.org/>.